Emissive Probes, Principles and Recent Developments

R. Schrittwieser[1], C. Ioniță[1], P.C. Balan[1], C.A.F. Varandas[2], C. Silva[2], J. Stöckel[3], M. Tichý[4], E. Martines[5], G. Van Oost[6], T. Klinger[7], R. Madani[7], R.M.O. Galvão[8], the ISTTOK team[2], the CASTOR team[3]

[1]*Association EURATOM/ÖAW, Department of Ion Physics, University of Innsbruck, Austria*

[2] *Association EURATOM/IST, Centro de Fusão Nuclear, Instituto Superior Técnico, Lisboa, Portugal*

[3]*Institute for Plasma Physics, Association EURATOM-IPP.CR, Czech Academy of Sciences, Prague, Czech Republic*

[4]*Faculty of Mathematics and Physics, Charles University in Prague, Czech Republic*

[5]*Consorzio RFX, Associazione EURATOM-ENEA sulla Fusione, Padova, Italy*

[6]*Department of Applied Physics, Ghent University, Belgium*

[7]*Max Planck Institute for Plasma Physics, Greifswald Branch, EURATOM Association, Germany*

[8]*Institute of Physics, University of São Paulo, São Paulo, Brasil*

roman.schrittwieser@uibk.ac.at

Abstract: An electron-emissive probe consists of a small electrode which can be heated until it starts to emit electrons. In a Maxwellian plasma, for increasing electron emission, the floating potential $V_{fl,em}$ approaches Φ_{pl}, attaining it in principle when the emission current equals the electron saturation current. This method does not require the knowledge of the electron temperature T_e, and also works for drifting electrons or electron beams. In this work first the principle method to measure the plasma potential Φ_{pl} by an emissive probe is discussed in general. Then also the question is treated why the floating potential of a strongly emissive probe can sometimes remain below the plasma potential. Finally the most recent developments on new probe types will be presented.

PACS: 52.70.Ds, 52.55.Fa, 52.25.Fi, 52.35.Ra

1. Introduction

The spatial profile and the temporal evolution of the plasma potential Φ_{pl} are decisive not only for the overall stability of a plasma but also for the loss of plasma confinement, in particular in the case of a magnetically confined plasma such as in toroidal fusion experiments. Very important in this context is the electric field and its fluctuations in the edge region since edge plasma turbulence can give rise to the fluctuation-induced radial particle flux and to important effects such as the Reynolds stress. In this context we would like to remind us that, through Poisson's equation, the plasma potential solely depends on the densities of the positive and negative charge carriers but not on the specific form of the velocity distribution functions, in particular not on particle drifts or beams.

In view of its relevance for such phenomena it is of utmost importance to gain as much as possible information on the behaviour of Φ_{pl}. Unfortunately, however, there are very few diagnostics which are able to measure this parameter with sufficient spatial and temporal resolution. There are intricate methods such as electron beams and heavy ion beams but these are not easily applicable in all types of plasma and are also expensive. Therefore the practically only diagnostic tools which permit a comprehensive determination of Φ_{pl} and, by use of probe arrays, of the electric field $\boldsymbol{E} = -\mathrm{grad}\,\boldsymbol{\Phi}_{pl}$, are plasma probes of various types and principles.

Plasma probes – in particular also emissive probes – have first been described by Langmuir and coworkers [1-3]. In spite of this fact "they have not found widespread use because of problems associated with strong electron emission and because of generally negative comments about them in previous review articles", as for instance Hershkowitz comments [4] on Chen [5].

In the original concept of emissive probes [5] a comparison was made between the current-voltage characteristic (*I-V* characteristic) of an emissive probe and of a cold probe (i.e., of the same probe unheated). The probe voltage where the emissive characteristic starts deviating from the cold one was considered to indicate the plasma potential.

Sellen et al. [6] and Kemp and Sellen [7] were among the first to use an electron-emissive probe (viz. a conventional wire probe) for systematic measurements of the plasma potential directly by using the floating potential method under strong electron emission. Another important, however, also indirect method was later described by Smith et al. [8], who argued that the inflection point of an emissive probe characteristic, at moderate emission current, yields a more precise measure for the plasma potential, moreover perturbing the plasma less. Later on, eminent contributions to the plasma diagnosis with emissive probes have been made especially by Hershkowitz and his group [9-14]. Other papers devoted mainly to the experimental and theoretical principles of emissive probes are [15-28]. Until the end of the 1990's emissive probes have been used almost exclusively in low-temperature plasma devices. As far as we know, the first successful applications of emissive probes in magnetic fusion experiments were reported in [25-28].

In the following, first the principle of an emissive probe will be discussed briefly (see also [4]). After that possible space charge effects will be treated [26]. In these cases, further surface effects, such as secondary electron emission, will be neglected. In the last section the conventional type of emissive probes and a newly developed emissive probe based on laser heating will be presented [29].

2. Determination of the plasma potential with cold and emissive probes

2.1. Cold probes

In a Maxwellian plasma, i.e., without drifting electrons or electron beams, the plasma potential can also be determined by means of cold probes. In this case the most accurate measure of Φ_{pl} is obtained from the inflection point of the characteristic, close to the "knee" where the electron saturation region commences. However, for the sake of simplicity it is usually assumed that Φ_{pl} can be inferred from the floating potential V_{fl} of a cold probe. For Maxwellian **v**elocity **d**istribution **f**unctions (VDF) of the ions and electrons, V_{fl} and Φ_{pl} are proportional to each other through the relation

$$\Phi_{pl} = V_{fl} + T_e \ln\left(\frac{I_{es}}{I_{is}}\right), \tag{1}$$

where T_e is the kinetic electron temperature and $I_{es,is}$ are the electron and ion saturation currents, respectively. So when T_e and V_{fl} are determined simultaneously, the plasma potential can in principle be calculated.

However, with temporal or spatial variations of T_e the calculation of $\Phi_{pl}(V_{fl})$ can become very complicated or even impossible. Also the effective areas of the probe for electron and ion collection, respectively, which are contained in $I_{es,is}$, can differ from each other, in particular in a magnetised plasma. In addition, stronger deviations of the electron VDF from a Maxwellian one (e.g. by an electron drift or beam) distort the *I-V* characteristic of a cold probe causing a shift of it to the negative side because of the kinetic energy of the electrons. Therefore a determination of the plasma potential from the "knee" of the characteristic can deliver erroneous results [25].

2.2. Emissive probes – saturated emission

These problems can partly be circumvented by the use of a probe, which emits an electron current into the plasma. An emission current I_{em} can flow from the probe to the plasma as long as the probe voltage V_p fulfils the condition $V_p \leq \Phi_{pl}$, *independently* of the plasma electron VDF and of fluctuations of T_e. For $V_p > \Phi_{pl}$, the emission current drops exponentially and electron collection begins to

dominate the probe current. Since the temperature of the emitted electrons T_{em} is usually much smaller than that of the plasma electrons, this exponential drop is very sharp. Therefore the floating potential $V_{fl,em}$ of an emissive probe can be taken as a sufficiently accurate approximation for the plasma potential [7].

In a purely Maxwellian plasma, for $V_p \le \Phi_{pl}$, the total current I_p to an emissive probe is [26]

$$I_p = I_{is} + I_{em} - I_{es}\exp\left(\frac{V_p - \Phi_{pl}}{T_e}\right). \tag{2}$$

At the floating potential, i.e. for $V_p = V_{fl,em}$, the total probe current I_p equals zero. Then, the difference between the floating and the plasma potential, normalized to T_e, is

$$\Delta \equiv \frac{\Phi_{pl} - V_{fl,em}}{T_e} = \ln\left(\frac{I_{es}}{I_{is} + I_{em}}\right), \tag{3}$$

which, for an unheated probe ($I_{em} = 0$) becomes simply:

$$\Delta = \ln\left(\frac{I_{es}}{I_{is}}\right) = \ln\left(\sqrt{\frac{T_e}{T_e + T_i}}\sqrt{\frac{m_i}{2\pi m_e}}\right) \equiv \Delta_0. \tag{4}$$

Here we have inserted the current densities for electrons and ions through the familiar relations $j_{es} = n_e e\sqrt{eT_e/2\pi m_e}$ and $j_{is} = n_i e\sqrt{e(T_e + T_i)/m_i}$, assuming equal effective areas of the probe for electron and ion collection (which is not always the case in a strongly magnetized plasma). The meanings of the symbols are $n_{e,i}$ for the electron and ion densities, respectively, $m_{e,i}$ for the electron and ion mass, respectively, and T_i for the kinetic ion temperature.

In order to derive a condition for the case when $V_{fl,em}$ of the probe corresponds to the plasma potential Φ_{pl}, we have to require $\Delta = 0$, and then we obtain from Eq. (3):

$$\frac{I_{es}}{I_{is} + I_{em}} = 1. \tag{5}$$

Again assuming equal collecting areas of the probe for electrons and ions, and inserting the above expressions for j_{es} and j_{is} into Eq. (5), we derive:

$$\frac{I_{em}}{I_{is}} = \frac{I_{es}}{I_{is}} - 1 = \sqrt{\frac{T_e}{T_e + T_i}}\sqrt{\frac{m_i}{2\pi m_e}} - 1 \tag{6}$$

Assuming further that $T_e = T_i$, for a hydrogen plasma, $I_{em}/I_{is} \cong 11$ and $I_{em}/I_{es} \cong 0.92$. The general behaviour of an emissive probe is seen from Eq. (3): For no probe heating, $I_{em} = 0$ and V_{fl} of the probe is that one of a cold probe. From Eq. (4), for typical edge plasma conditions of a smaller tokamak ($T_e = T_i = 10$ eV in energy units) and for a hydrogen plasma, we obtain $\Delta_0 = 2.5$, i.e., V_{fl} is smaller than Φ_{pl} by $2.5T_e$. For increasing probe heating, I_{em} increases, which means that Δ becomes smaller (see Eq. 3), and the floating potential of the probe increases and approaches Φ_{pl} until for $I_{em}/I_{es} \cong 0.92$, $V_{fl,em} \cong \Phi_{pl}$.

Whereas Eq. (3) indicates that for stronger heating $V_{fl,em}$ becomes larger than Φ_{pl}, in reality the floating potential of a sufficiently emissive probe does not surpass Φ_{pl}, since our simplified treatment is valid only for $V_p \le \Phi_{pl}$.

Fig. 1 shows a comparison between the theoretical behaviour of Δ as a function of I_{em}/I_{is} (Fig. 1a), according to Eq. (3), and results from an experiment where an emissive probe has been used in the edge region of the CASTOR tokamak (**C**zech **A**cademy of **S**cience **Tor**us) (Fig. 1b, for two radial positions in the edge region of CASTOR [26]), where the density was about 10^{18} m^{-3} and $T_e \cong$

10 eV. CASTOR has a major radius of 40 cm and a minor radius of about 8.5 cm. The typical magnetic field is 1 T and the usual plasma current 10 kA.

In both cases (Fig. 1a and b) we see that Δ (here shown negative for better clarity) starts from a certain value for no heating (i.e. when the probe is cold and V_{fl} is, as usual, more negative than Φ_{pl}), becomes smaller for increasing heating and approaches zero where the floating potential $V_{fl,em}$ is supposed to be equal to the plasma potential. In theory this occurs, as we have seen above, for $I_{em}/I_{is} \cong 11$.

We see that the experimental results (Fig. 1b) show a similar behaviour, except that in this case $V_{fl,em}$ saturates better. The saturated value is called $V^*_{fl,em}$. Also this saturation begins at about $I_{em}/I_{is} \cong 11$. There is, however, a discrepancy concerning the starting point of the curves: in the theoretical case $\Delta = \Delta_0 = 2.5$, as mentioned above. But in the experiment Δ_0 seems to be about 1.4. We can, however, not be sure about the correct calibration of the *y*-axis, which means that the final value of $V_{fl,em} = V^*_{fl,em}$ might not yet really corresponds to Φ_{pl}, but there might still be a difference between the saturated emissive probe floating potential and the plasma potential. For an explanation of this effect, see the next section.

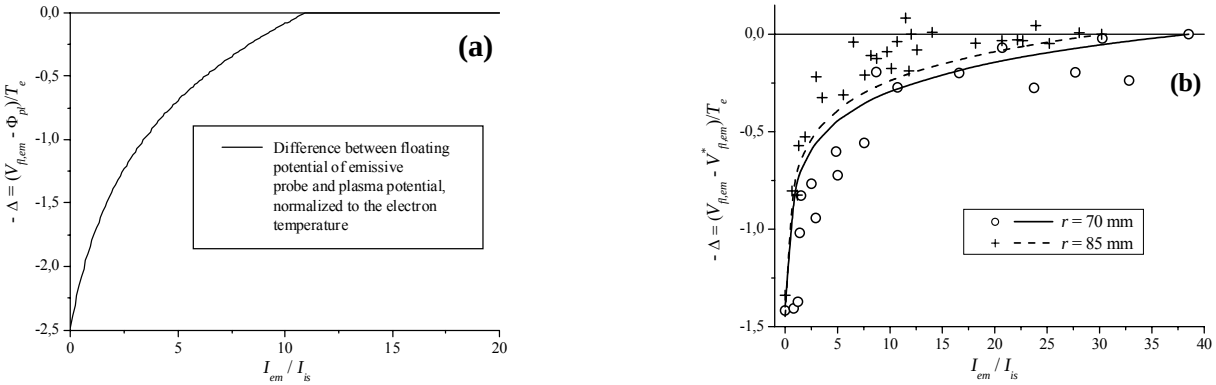

Fig.1. (a) Theoretical behaviour of the normalised difference between the floating and the plasma potential of an emissive probe according to Eq. (3) vs. normalised emission current; (b) Analogous experimental results from the CASTOR tokamak in Prague at two radial positions in the edge plasma region [26].

2.3. Emissive probes – space charge limited emission

The treatment above is valid as long as space charge effects by the emitted electrons can be neglected. However, the emitted electrons have usually a lower temperature (namely that of the wire which is about $T_w \leq 0.2$ eV) than that of the plasma electrons ($T_e \cong 0.2$ - 100 eV, depending on the plasma type). Therefore the former usually have also a lower average current density than the plasma electrons. Thus for $V_{fl,em} = \Phi_{pl}$, the current of the plasma electrons towards the probe would be much larger than that of the emitted electrons away from it, and the probe would not really be floating. Compared to these currents, the ion current can be neglected. As a reaction, an electron-rich sheath is built up around the probe by the emitted electrons [22-24], by which $V_{fl,em}$ drops from Φ_{pl} to a somewhat lower value. By this potential difference the plasma electrons are partly prevented from the probe, whereas the emitted electrons are accelerated, thereby reconstituting the equilibrium between the two electron currents towards the probe and away from it, and re-establishing the floating condition. This has the effect that $V_{fl,em}$ does not attain the plasma potential completely but would stay below it, as it appears also from Fig. 1b.

This effect has been mentioned by several earlier authors (see e.g. [5,17]) but only recently it has been described by numerical [22] and theoretical models [23,24]. Obviously, such an effect impairs the accuracy of the determination of Φ_{pl} and has therefore to be investigated thoroughly to clarify under which conditions it appears, what it depends on and how it can be taken into account.

In such a case, in Eq. (3) for I_{em} not the saturated electron emission current according to Richardson's emission law has to be inserted, but a space charge limited current, considering the system probe-plasma as an electron diode with the probe as hot cathode and the plasma as anode. To get an approximate idea about this effect, in Eq. (2) we replace I_{em} by the Child-Langmuir current

$$I_{CL}(V_p) = A_{em}\frac{4\varepsilon_0}{9}\left(\frac{2e}{m_e}\right)^{1/2}\frac{(\Phi_{pl}-V_p)^{3/2}}{d^2}, \tag{7}$$

where A_{em} is the probe area effective for electron emission and d is the sheath thickness. In case of an emissive probe in a plasma, we assume d to be around the Debye length, thus $d = \lambda_{De}$. Therewith, at the floating potential $V_{fl,CL}$, Eq. (7) becomes

$$I_{CL}(V_{fl,CL}) = A_{em}\frac{4n_e e}{9}\left(\frac{2eT_e}{m_e}\right)^{1/2}\left[\frac{\Phi_{pl}-V_{fl,CL}}{T_e}\right]^{3/2}. \tag{8}$$

Equating the total probe current to zero, Eq. (2) for this case becomes

$$0 = I_{is} - I_{es}\exp\left[-\frac{\Phi_{pl}-V_{fl,CL}}{T_e}\right] + I_{CL}(V_{fl,CL}). \tag{9}$$

We emphasise that in this case $V_{fl,CL}$ does not depend on the emission current and that for $\Phi_{pl} = V_{fl,CL}$ there would be no emission current at all. Of course, this is not realistic, but may serve as a first simplifying assumption. In analogy to Eq. (3) we define

$$\Delta_{CL} \equiv \frac{\Phi_{pl}-V_{fl,CL}}{T_e}. \tag{10}$$

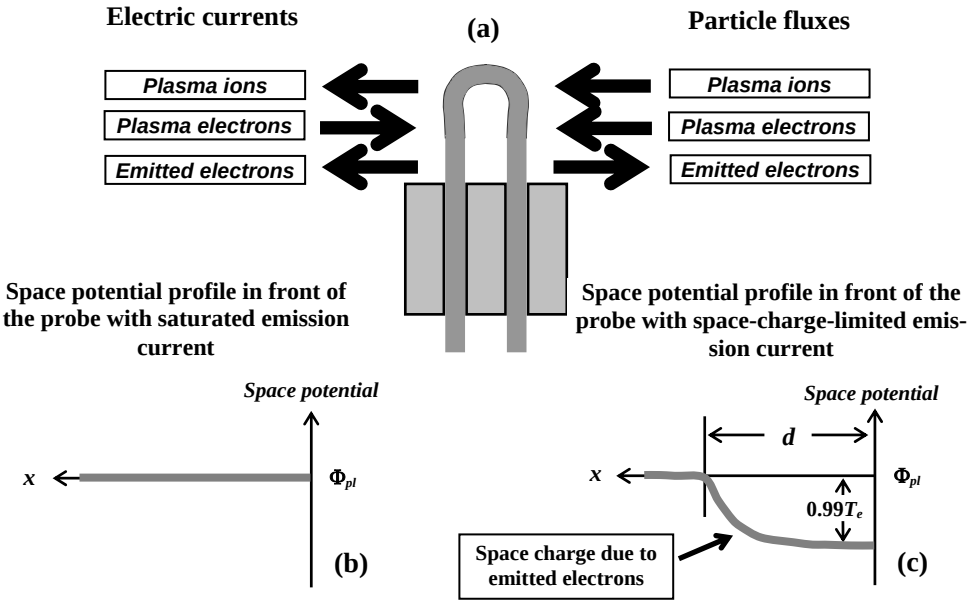

Fig.2. (a) Schematic of the electric currents (left) and the particle fluxes (right) around an emissive probe; (b) Saturated emission case, where no negative space charge is formed around the probe; (c) Space charge limited case where the emitted electrons form a space charge, which leads to a difference between the potential of the floating probe and the plasma potential.

For further analysis it will be useful to normalise the Child-Langmuir current to the electron saturation current I_{es}. Therewith we obtain

$$\frac{I_{CL}}{I_{es}} = \frac{A_{em}}{A_e}\frac{2\sqrt{\pi}}{9}\Delta_{CL}^{3/2} \equiv K\Delta_{CL}^{3/2}, \tag{11}$$

with A_e being the probe area effective for electron collection and $K \equiv \left(2\sqrt{\pi}/9\right)\left(A_{em}/A_e\right)$. Using Eqs. (10) and (11), Eq. (9) becomes

$$\frac{I_{is}}{I_{es}} + K\Delta_{CL}^{3/2} - \exp\left(-\Delta_{CL}\right) = 0. \tag{12}$$

For $A_{em}/A_e = 1$, the solution of this equation delivers $\Delta_{CL} \cong 0.99$. This means that the floating potential of the emissive probe saturates at about one T_e below the true value of the plasma potential, due to the formation of a space charge around it. This seems also to be the case for the results shown in Fig. 1b, where Δ_0 for no probe heating is 1.4, whereas according to the theory this should be 2.5. Therefore the graphs of Fig. 1b can also be interpreted in such a way that the saturated value of $V_{fl,em}$ does not reach the true value of Φ_{pl} but is stuck underneath by about T_e.

Fig. 2a shows the electric currents and the particle fluxes around an emissive probe schematically and a comparison of the space potential profiles between the case without space charge (Fig. 2b on the left), where the emissive current is saturated, and the latter case (Fig. 2c on the right), where a double layer is formed around the probe consisting of a negative space charge layer around the probe, produced by emitted electrons, and of a positive layer for the adjustment to the plasma potential at larger distances from the probe.

3. Construction of emissive probes, recent developments and results

3.1. Conventional emissive wire probe

A typical emissive wire probe, as it was used in the experiments in tokamaks [25-27], consists of a ceramic tube (Al_2O_3) with an oval cross-section of 1.4×2.3 mm outer dimensions and a length of about 7 cm. The Al_2O_3 tube has two bores of 0.7 mm diameter each. Through them a 0.2 mm diameter tungsten wire is inserted in such a way that on the "hot end" a W-wire loop of about 6 mm length is formed. Inside both of the bores, the W-wire extends about 3 cm towards the "cold end" of the ceramic tube. Before the insertion, each W-wire is spliced twice with about 12 copper threads with diameters of 0.05 mm [25,26]. In this way, inside the bores the W-wires are covered with a layer of Cu. This treatment has the effect that only the exposed loop of the emissive probe is heated when a current is passed through. By careful choice of the number of Cu-threads, by which the W-wire is wrapped, the thickness of the combined wires can be adjusted so that they tightly fit into the bores of the Al_2O_3 tube. This provides an excellent contact between the two materials, which can otherwise not be soldered or welded together. In addition, on the cold side the twisted copper threads provide an excellent connection to the electrical leads to the feed-throughs and to the external power supply or battery. Fig. 3 shows a schematic of an emissive wire probe in the plasma together with the necessary heating circuit.

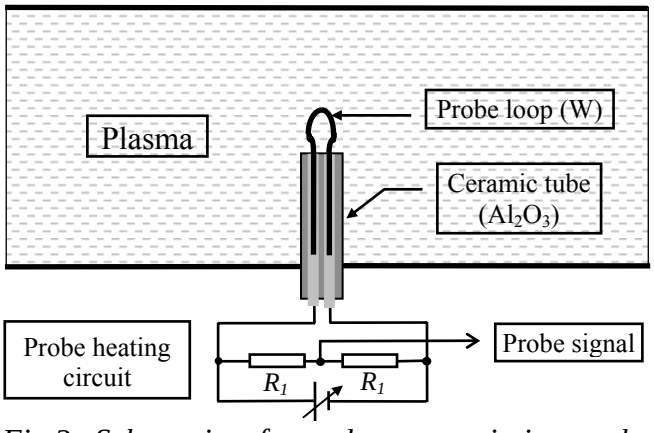

Fig.3. Schematic of an electron emissive probe with the heating circuit; the two resistors R_1 are identical and balance the voltage drop of the heating current over the probe loop. After determining the necessary value of $I_{em} \geq I_{es}$ by adjusting the heating current, the floating potential of the heated probe is assumed to be a sufficient approximation of the plasma potential.

When such a probe is heated and electron

emissions starts, the *I-V* characteristic begins to show the electron emission current as superimposed on the ion saturation current on the left-hand side. At the same time, also the floating potential $V_{fl,em}$ starts to shift to the right. For strong emission, $V_{fl,em}$ reaches a saturation and no further shift to the right occurs. This saturated value $V^*_{fl,em}$ is assumed to be a good approximation to the plasma potential, albeit we have always to take into account the considerations of subsection 2.3. above.

3.2. Arrangements of emissive and cold probes

Fig. 4a shows an example of an arrangement of emissive and cold probes, used in a tokamak for the determination of electric field fluctuations. With this set-up, in ISTTOK (**I**nstituto **S**uperior **T**écnico **Tok**amak, Lisbon) the fluctuations of the radial and poloidal electric fields, $\widetilde{E}_{r,\vartheta}$, have been measured simultaneously in the edge plasma region [28]. The additional cold probe served for measuring the plasma density fluctuations $\widetilde{n}_{pl} \cong \widetilde{n}_i$ via the ion saturation current, neglecting fluctuations of T_e. ISTTOK is a tokamak with very similar parameters as CASTOR mentioned above.

These data were used to calculate on one side the radial fluctuation-induced particle flux $\Gamma_r = \left\langle \widetilde{n}_{pl}\widetilde{v}_r \right\rangle \cong \left\langle \widetilde{n}_{pl}\widetilde{E}_\vartheta \right\rangle / B$, and on the other side the Reynolds stress $R_e = \left\langle \widetilde{v}_r \widetilde{v}_\vartheta \right\rangle \cong \left\langle \widetilde{E}_\vartheta \widetilde{E}_r \right\rangle / B^2$ [28]. Fig. 4b shows a typical probability distribution function (PDF) of Γ_r. The grey curve shows the case when the three probes were unheated. In this case, the cold probe floating potentials V_{fl} were used as approximations for the plasma potentials, which means that also temperature fluctuations had an influence on the values of V_{fl}. The black curve has been obtained with the probes heated to electron emission so that a better approximation of the plasma potential was used as a basis for calculating Γ_r, with the influence of T_e-fluctuations minimized. The PDF determined with the emissive probes is narrower but it also shows a more non-Gaussian character than that determined with the cold probes. This can be seen by comparison with the respective Gaussian PDFs that are also shown in the figure. A non-Gaussian PDF is a sign for a stronger radial transport into one direction, which in this case is obviously the direction outward.

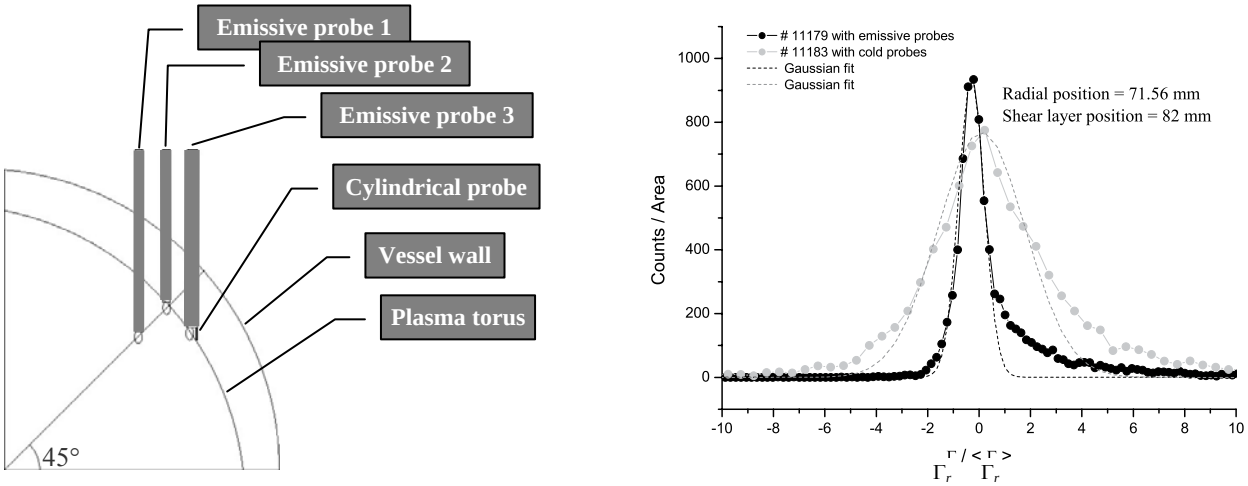

Fig.4. (a) Poloidal view of the experimental set-up in ISTTOK [28]; (b) Probability distribution function (PDF) of the radial particle flux in the edge plasma region, once determined by the three probes unheated (grey) and once heated (black). The black and grey dotted lines show the corresponding fitted Gaussians.

3.3. Laser-heated emissive probe

In a recent investigation at the VINETA plasma machine at the Max Planck Institute, Greifswald Branch, Germany [29] a laser-heated emissive probe was developed. Only in two earlier works a laser system was mentioned for heating a wire probe [30, 31].

The VINETA produces an argon plasma column of 10 cm diameter and 4 m length in a magnetic

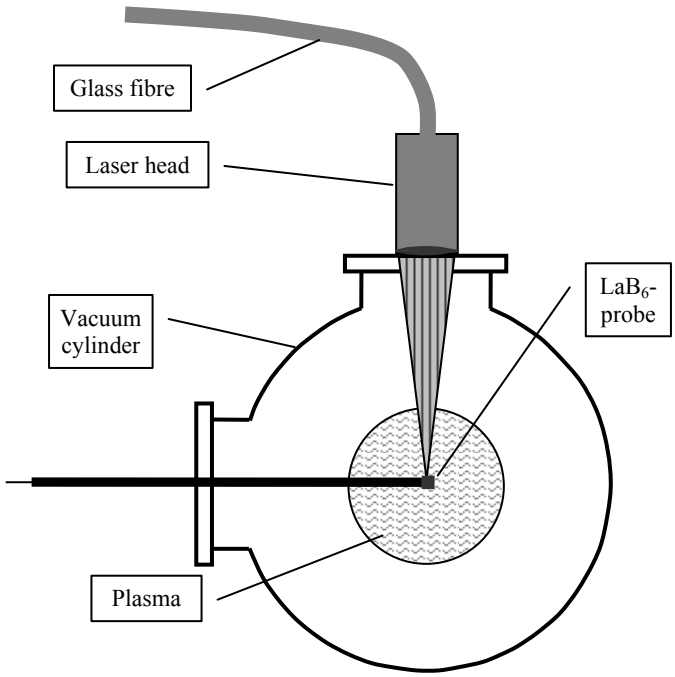

Fig.5. Cross-section through the VINETA device with the laser-heated probe system.

field of 0.1 T with a density of about 10^{19} m^{-3}, an electron temperature of 3 eV and an ion temperature of 0.2 eV. The plasma is produced by a helicon discharge of less than 6 kW [32].

The probe consists of a disc of lanthanum hexaboride, LaB_6, with a diameter of 3.2 mm and a height of 2.2 mm. The LaB_6 electrode is connected to a molybdenum wire of 0.2 mm diameter pulled through a ceramic tube for electrical connection. The LaB_6 electrode is heated by an infrared high-power diode laser JenLas HDL50F from JenOptik, Jena, Germany, with a maximum output power of 50 W and a wavelength of 808 nm. The laser beam is coupled to a glass fibre of about 3 m length that ends in a lens head, by which, in a distance of 15 cm, a focus of 0.6 mm diameter can be produced. This laser-head was set directly on a quartz-glass window perpendicular to the probe. Fig. 5 presents a cross-section through the VINETA machine, showing this set-up schematically.

From Fig. 6a we see that also the laser-heated emissive probe shows the typical behaviour as a conventional emissive wire probe (Fig. 1b), i.e., for increasing laser-heating power P_L the emission current supersedes the ion saturation current while $V_{fl,em}$ shifts to more positive values. The inserted values of T_e = 4.12 eV and Φ_{pl} = +11.6 V, have been determined from the cold *I-V* characteristic (for P_L = 0 W) for comparison. Fig. 6b is the analogue to Fig. 1b by showing the variation of $V_{fl,em}$ with the laser heating power. Starting from the floating potential $V_{fl} \cong -3.3$ V (which corresponds to $\Delta \cong 3.6$) of the same but cold probe, with increasing heating power the floating potential rises. At a laser power of $P_L \cong 13$ W, $V_{fl,em}$ jumps up and reaches a final saturation of $V^*_{fl,em}$ = +8.8 V for $P_L \geq$ 40 W, which corresponds to $\Delta \cong 0.68$. This value lies about 2.9 T_e above V_{fl}, thus $\Delta_0 \cong 2.9$. We emphasize that in this case (in contrast to Fig. 1b) Δ has the same meaning as in the theoretical case (see Fig. 1a), i.e., the difference between the actual value $V_{fl,em}$ and Φ_{pl} = 11.6 V determined from the characteristic of the unheated probe. Again we observe that the saturated value of $V^*_{fl,em}$ remains below the value of Φ_{pl} determined from the cold characteristic.

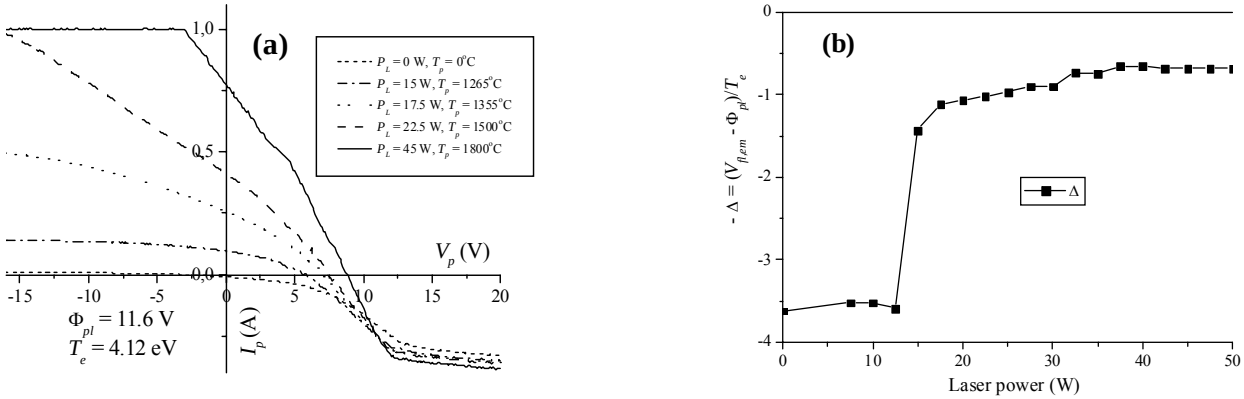

Fig.6. (a) Typical probe characteristics from VINETA for increasing probe heating by laser irradiation; the laser power and the corresponding temperature of the probe are indicated; (b) Approach of the floating potential of the laser heated emissive probe to the plasma potential versus the laser heating power.

As in the case of the emissive wire probe (section 3.1., Fig. 1b), this discrepancy is ascribed to the formation of negative space charge sheath around the emissive probe [24]. However, in contrast to the emissive wire probe in CASTOR, here $V^{*}_{fl,em}$ lies only about $0.68\,T_e$ below Φ_{pl}. This is in better agreement with the simulations by Reinmüller [22].

4. Conclusion

We have discussed the principle and various types of emissive probes, which can even be used in the edge region of smaller toroidal fusion experiments. With such probes also the temporal development of the plasma potential can be recorded including fluctuations, and arrangements are possible, by which the electric field in various directions can be determined directly [27,28]. A certain perturbation of the plasma by such a probe can unfortunately not be avoided. But this depends also on the size of the probes and can still be further improved. We envisage the use of such emissive probes even for larger fusion experiments such as TJ-II and ASDEX Upgrade.

Acknowledgements

This work has been carried out within the Associations EURATOM-ÖAW, EURATOM-IST, EURATOM-IPP.CR and EURATOM-IPP (Greifswald Branch). The content of the publication is the sole responsibility of its author(s) and it does not necessarily represent the views of the Commission or its services. The support by the Fonds zur Förderung der wissenschaftlichen Forschung (Austria) under grant No. P-14545 is acknowledged. The work was further supported by grant GA ČR 202/03/0786 (probe construction) and project AV K2043105 (tokamak operation), partially by INTAS project No. 2001-2056.

References

1. H. M. Mott-Smith, I. Langmuir. *The theory of collectors in gaseous discharges*, Phys. Rev. **28** (1926) 727-763.
2. I. Langmuir. *The interaction of electron and positive ion space charges in cathode sheaths*, Phys. Rev. **33** (1929), 954-989.
3. I. Langmuir, K.T. Compton. *Electrical discharges in gases part II. Fundamental phenomena in electrical discharges*, Rev. Mod. Phys. **3** (1931) 191-257.
4. N. Hershkowitz. *How Langmuir probes work*, Chapter 3 of *Plasma Diagnostics, Vol. 1 (Discharge Parameters and Chemistry)* (Ed. O. Auciello and D.L. Flamm), Academic Press, (1989) 113-183.
5. F.F. Chen. *Electric probes*, Chapter 4 of *Plasma diagnostic techniques* (R.H. Huddlestone and S.L. Leonard), Academic Press, (1965) 113-200.
6. J.M. Sellen Jr., W. Bernstein, R.F. Kellen. *Generation and diagnosis of synthesized plasma streams*, Rev. Sci. Instrum. **36** (1965) 316-322.
7. R.F. Kemp, J.M. Sellen Jr.. *Plasma potential measurements by electron emissive probes*, Rev. Sci. Instrum. **37** (1966) 455-461.
8. J.R. Smith, N. Hershkowitz, P. Coakley. *Inflection-point method of interpreting emissive probe characteristics*, Rev. Sci. Instrum. **50** (1979) 210-218.
9. M.H. Cho, C. Chan, N. Hershkowitz, T. Intrator. *Measurement of vacuum space potential by an emissive probe*, Rev. Sci. Instrum. **55** (1984) 631-632.
10. E.Y. Wang, T. Intrator, N. Hershkowitz. *Direct indication technique of plasma potential with differential emissive probe*, Rev. Sci. Instrum. **56** (1985) 519-524.
11. E. Y. Wang, N. Hershkowitz, T. Intrator, C. Forest. *Techniques for using emitting probes for potential measurement in rf plasmas*, Rev. Sci. Instrum. **57** (1986) 2425-2431.

12. D. Diebold, N. Hershkowitz, A. D. Bailey III, M. H. Cho, T. Intrator. *Emissive probe current bias method of measuring dc vacuum potential*, Rev. Sci. Instrum. **59** (1988) 270-275.
13. N. Hershkowitz, M.H. Cho. *Measurement of plasma potential using collecting and emitting probes*, J. Vacuum Sci. Technol. A **6** (1988) 2054-2059.
14. T. Lho, N. Hershkowitz, G-H. Kim. *Effect of harmonic rf fields on the emissive probe characteristics*, Rev. Sci. Instrum. 71 (2000) 403-405.
15. K. Hirao, K. Oyama. *Measurement of the space potential in plasma*, J. Geomagn. Geoelectr. **23** (1971) 47-60.
16. R.W. Motley. *Hot-probe measurements of space potential oscillations in a plasma*, J. Appl. Phys. **43** (1972) 3711-3716.
17. J.J. Schuss, R.R. Parker. *Behavior of electron-emitting plasma probes in the space-charge-limited regime*, J. Appl. Phys. **45** (1974) 4778-4783.
18. S. Iizuka, P. Michelsen, J.J. Rasmussen, R. Schrittwieser, R. Hatakeyama, K. Saeki, N. Sato. *A method for measuring fast time evolutions of the plasma potential by means of a simple emissive probe*, J. Phys. E: Sci. Instrum. **14** (1981) 1291-1295.
19. R.L. Merlino, S.L. Cartier. *The perturbing effect of a Langmuir probe near a magnetised double layer*, J. Phys. D: Appl. Phys. **20** (1987) 1074-1076.
20. A. Siebenförcher, R. Schrittwieser. *A new simple emissive probe*, Rev. Sci. Instrum. **67** (1996) 849-850.
21. S. Yan, H. Kamal, J. Amundson, and N. Hershkowitz. *Use of emissive probes in high pressure plasma*, Rev. Sci. Instrum. **67** (1996) 4130-4137.
22. K. Reinmüller. *Determination of the plasma potential using emissive probes – implications from PIC simulations*, Contrib. Plasma Phys. **38** (1998) 7-12.
23. S. Takamura, M.Y. Ye, T. Kuwabara, N. Ohno. *Heat flows through plasma sheaths*, Phys. Plasmas **5** (1998) 2151-2158.
24. M.Y. Ye, S. Takamura. *Effect of space-charge limited emission on measurements of plasma potential using emissive probes*, Phys. Plasmas **7** (2000) 3457-3463.
25. R. Schrittwieser, C. Ioniță, P.C. Balan, Jose A. Cabral, H.F.C. Figueiredo, V. Pohoață, C. Varandas. *Application of emissive probes for plasma potential measurements in fusion devices*, Contrib. Plasma Phys. **41** (2001) 494-503.
26. R. Schrittwieser, J. Adámek, P. Balan, M. Hron, C. Ioniță, K. Jakubka, L. Kryška, E. Martines, J. Stöckel, M. Tichý, G. Van Oost. *Measurements with emissive probes in the CASTOR tokamak*, Plasma Phys. Contr. Fusion **44** (2002) 567-578.
27. P. Balan, R. Schrittwieser, C. Ioniță, J.A. Cabral, H.F.C. Figueiredo, H. Fernandes, C. Varandas, J. Adámek, M. Hron, J. Stöckel, E. Martines, M. Tichý, G. Van Oost. *Emissive probe measurements of the plasma potential fluctuations in the edge of the ISTTOK and CASTOR tokamaks*, Rev. Sci. Instrum. **74** (2003) 1583-1587.
28. C. Ioniță, P. Balan, R. Schrittwieser, H.F.C. Figueiredo, C. Silva, C.A.F. Varandas, R.M.O. Galvão. *An arrangement of emissive probe and cold probes for fluctuation and Reynolds stress measurements*, Rev. Sci. Instrum., in print.
29. R. Madani, C. Ioniță, R. Schrittwieser, G. Amarandei, P. Balan, T. Klinger. *A laser-heated emissive probe for fusion applications*, Proc. 31st EPS Conf. Plasma Phys. (London, Great Britain, 2004), in print.
30. S. Ono, S. Teii. *Laser-heated emission of electrons from a carbon-coated metal surface and its application to the emissive probe measurements*, Rev. Sci. Instrum. **50** (1979) 1264-1267.
31. M. Mizumura, S. Uotsu, S. Matsumura, S. Teii, *Probe system with bias compensation using a laser heated emissive probe for RF discharge plasma diagnostics*, J. Phys. D: Appl. Phys. **25** (1992) 1744-1748.
32. C.M. Franck, O. Grulke, T. Klinger. *Mode transitions in helicon discharges*, Phys. Plasmas **10** (2003) 323-325.